

Kim, Yunsun; Son, Heung-gu; Kim, Sahm

Article

Short term electricity load forecasting for institutional buildings

Energy Reports

Provided in Cooperation with:

Elsevier

Suggested Citation: Kim, Yunsun; Son, Heung-gu; Kim, Sahm (2019) : Short term electricity load forecasting for institutional buildings, Energy Reports, ISSN 2352-4847, Elsevier, Amsterdam, Vol. 5, pp. 1270-1280,
<https://doi.org/10.1016/j.egyr.2019.08.086>

This Version is available at:

<https://hdl.handle.net/10419/243668>

Standard-Nutzungsbedingungen:

Die Dokumente auf EconStor dürfen zu eigenen wissenschaftlichen Zwecken und zum Privatgebrauch gespeichert und kopiert werden.

Sie dürfen die Dokumente nicht für öffentliche oder kommerzielle Zwecke vervielfältigen, öffentlich ausstellen, öffentlich zugänglich machen, vertreiben oder anderweitig nutzen.

Sofern die Verfasser die Dokumente unter Open-Content-Lizenzen (insbesondere CC-Lizenzen) zur Verfügung gestellt haben sollten, gelten abweichend von diesen Nutzungsbedingungen die in der dort genannten Lizenz gewährten Nutzungsrechte.

Terms of use:

Documents in EconStor may be saved and copied for your personal and scholarly purposes.

You are not to copy documents for public or commercial purposes, to exhibit the documents publicly, to make them publicly available on the internet, or to distribute or otherwise use the documents in public.

If the documents have been made available under an Open Content Licence (especially Creative Commons Licences), you may exercise further usage rights as specified in the indicated licence.



<https://creativecommons.org/licenses/by/4.0/>



Research paper

Short term electricity load forecasting for institutional buildings

Yunsun Kim^a, Heung-gu Son^b, Sahm Kim^{c,*}^a Department of Applied Statistics, Chung-ang University, Seoul, Korea^b Korea Power Exchange, Naju, Korea^c Department of Applied Statistics, Chung-ang University, 84 Heukseok-ro, dongjak-gu, Seoul 06974, Korea

ARTICLE INFO

Article history:

Received 9 January 2019

Received in revised form 9 August 2019

Accepted 31 August 2019

Available online xxxx

Keywords:

Peak load demand forecasting

Institutional building

Time series

ARIMA

GARCH

ANN

ABSTRACT

Peak load demand forecasting is important in building unit sectors, as climate change, technological development, and energy policies are causing an increase in peak demand. Thus, accurate peak load forecasting is a critical role in preventing a blackout or loss of energy. This paper presents a study forecasting peak load demand for an institutional building in Seoul. The dataset were collected from campus area consisting of 23 buildings. ARIMA models, ARIMA-GARCH models, multiple seasonal exponential smoothing, and ANN models are used. We find an optimal model with moving window simulations and step-ahead forecasts. Also, including weather and holiday variables is crucial to predict peak load demand. The ANN model with external variables (NARX) worked best for 1-h to 1-d ahead forecasting.

© 2019 The Authors. Published by Elsevier Ltd. This is an open access article under the CC BY license (<http://creativecommons.org/licenses/by/4.0/>).

1. Introduction

Peak load demand forecasting is a critical issue at the national scale for smaller-scale building units (residential, commercial, and industrial) (Yao et al., 2003; Kavousian et al., 2013). As nations face the onslaughts of rapid climate change, record-breaking high temperatures have resulted in hotter summers. On the other hand, extreme cold temperatures have led to colder winters. Therefore, the number of buildings that use air-conditioners and heating appliances as necessities are bound to increase every year, and the frequency of their use is also set to rise. As these energy-intensive devices are responsible for a large portion of peak load demand, this demand continues to set new records every year. Therefore, simulation studies on the energy consumption of buildings are being actively conducted as a result of climate change (Santamouris et al., 2001).

Certain appliances have been commercialized within the span of a few decades. The invention of the electric vehicle (EV) is one such example; it is expected that EVs will become a necessity for each household as they replace vehicles run on fossil fuels in the near future. Thus, charging stations for EV have already been installed in some commercial or industrial buildings. It is thus predicted that the increasing number of EVs is likely to add to the already huge peak load demand in the building sector. Some researchers have shown this incremental trend in peak load demand as the EV market continues to grow, suggesting the

importance of load demand forecasting for buildings (Habib et al., 2015).

In addition, energy policies are being discussed to replace nuclear power, which used to provide a large proportion of power, with renewable energy (RE) (Renn and Marshall, 1950). Nuclear power is inexpensive to produce and generates high power output, but it suffers from disadvantages in that it is sensitive to management practices and even a single accident can have a severe negative impact on the environment. Thus, the future role of RE in satisfying peak load demand is bound to become stronger due to the controversies over nuclear power generation. Therefore, accurate peak load demand forecasting should be based on the national energy supply policy, which should focus on determining RE supply.

The energy relative prices and power rates can be set on the results of peak load demand forecasting in the near term. Besides, it was reported that the government of Korea made a decision in 8th basic Plan for Power Supply and Demand to reduce coal-fired and nuclear plant capacity and replace with RE and LNG, based on the results of the predicted demand, that is expected to decrease from a long-term point of view (Ministry of Trade, 2017). This not only affects a country's policies and economy, but also environmental conventions such as reducing fine dust and carbon dioxide emissions worldwide.

Due to technological advances, such as those witnessed for the smart grid and information and communications technologies (ICT), the subject of forecasting electric power demand is not limited to energy suppliers or energy policy legislators, but extends to building owners or managers of commercial, industrial, and residential buildings. The smart grid technology has

* Correspondence to: Department of Applied Statistics, Chung-ang University, 84 Heukseok-ro, dongjak-gu, Seoul 06974, Korea.

E-mail address: sahm@cau.ac.kr (S. Kim).

increased the efficiency of power demand and supply by exchanging information between power suppliers and end-users with smart meters. Before the smart grid was invented, a top-down approach, which was governed by economic considerations of the government with regard to the supply side, was implemented using aggregated data. However, currently, the top-down approach is not ideal for forecasting. Instead, the bottom-up approach, which involves engineering, considers the end-users' requirements, and concerns demand side management, has become popular with the advent of smart grid technology (Reyna and Chester, 2017). Thus, in the past, the top-down approach was suitable for short-term forecasting (Dahl et al., 2018), whereas today, the bottom-up approach has become widely applicable for the same task (Ghedamsi et al., 2016). Also, as information is provided in real time to consumers and suppliers, the demand response policy has ushered in a new paradigm of energy efficiency and forecasting (Rahimi and Ipakchi, 2010). Accurate STLF helps utilities and providers address the tasks caused by renewable penetration and electricity market development with complex pricing strategies in future smart grid markets.

Thus, climate change, technological development, and prevailing energy policies are likely to cause a sudden increase in peak demand, and demand forecasts need to be undertaken at the consumers' end. Accurate load forecasting is important to prevent possible loss of energy, because forecast underestimation can cause a blackout, whereas overestimation would result in energy wastage.

Forecasting methods are classified in various ways depending on the research objectives and methodology used. Forecasting can be categorized as short-, medium-, and long-term forecasting based on the time horizon. Depending on the concerned building sector, forecasts can be categorized as those for the residential, commercial, or industrial sector. Lastly, the methodology used to make the forecast can be classified as a traditional statistical or non-statistical method (Amjady, 2001).

Also, for the institutional building (see Section 4), this study demonstrates an optimal model for certain k time units with moving window simulations through 1 to 24 step-ahead forecasts.

After a review of the variable prediction studies, we compared the effectiveness of forecasting peak load demand for an institutional building using statistical and artificial intelligence (AI)-based models under various scenarios including exogenous variables. The contributions of this paper are presented as follows.

- (1) To the best of the authors' knowledge, there was no paper comparing and analyzing multiple statistical models and AI-based models in comprehensive ways. The results may provide different insights into which models are optimal with and without additional input data, not concluding that models with external variables are regarded as absolute truth in all models.
- (2) Various scenarios over prediction horizons are carried out through an hour to a day ahead forecasting. The results propose forecasting framework according to their forecasting horizons for robust and universal criterion.

The remainder of this paper is organized as follows. Section 2 provides a literature review of the types of models used for forecasting energy demand. Section 3 introduces the models used in this study. Section 4 illustrates the data and variables. Section 5 applies the data to the models described in Section 3, and Section 6 presents the performance evaluations of the same. Section 7 concludes the paper.

2. Literature review

While no standard time horizon period exists, it is common to set a period of a week or less for short-term forecasts (STLF), a week to months for a medium-term forecast (MTLF), and a year or more for a long-term forecast (LTFL) (Hong and Fan, 2016). Research on STLF has been conducted actively but requires a bottom-up approach. Boroojeni et al. (2017) analyzed STLF for different cycles of seasonality using hourly metered load data. Amjady (2001) suggested a solution for identifying the daily peak load by differentiating the dataset in terms of daily characteristics. MTLF plays an important role in planning and operating power generation systems. Dehghanzadeh et al. (2018) proposed a MTLF method to deal with weekly nonindustrial load. LTFL is commonly used as a top-down approach for planning by power generation facilities and transmission systems or addressing energy policy and legislation (Hong and Fan, 2016). Hyndman (Hyndman and Fan, 2010) proposed a density forecasting methodology to estimate probability distributions of peak load demand in order to overcome uncertainties in LTFL. Ekonomou (2010) described using an artificial neural network (ANN) model to forecast long-term national energy consumption in Greece.

Many sectoral studies exist as well as the end-users for each sector have different characteristics with regard to peak demand. In particular, as bottom-up approaches are preferred, appropriate modeling techniques should be applied so as to match each energy sector's specific characteristics. First, studies on the residential sector should consider various geographical and environmental factors, including the main appliances used by end-users and their living patterns, which would affect the peak load demand. Also, as the household penetration rate for the smart meter increases, it would become easier to access real-time measurements for short-term forecasting for the residential sector. Ghofrani et al. (2011a) examined a short-term forecasting method for residential customers using the smart grid via Kalman filtering. They considered different sampling periods and time horizons. Fan et al. (2017) modeled residential peak demand in Sydney using smart grid data including housing information from surveys. Kavousian et al. (2013) suggested relevant factors to consider residential load forecasting using factor analysis. It was shown that high-energy consumption appliances such as air-conditioners easily influence peak load demand. Thus, they noted that climate-related effects should be considered in the model. Pielow et al. (2012) predicted energy consumption in the industrial sector using an ANN model and inputs of yearly values from the industrial, residential, agricultural, and transportation sectors.

As stated previously, forecasting techniques can be classified into two major types: traditional statistical models and AI-based models. Classic models use mathematical combinations of historical data, and the estimates of parameters in such models can be easily interpreted. Examples include the Auto Regressive Integrated Moving Average (ARIMA) model (Amjady, 2001; Lazos et al., 2014; Jung and Kim, 2014), the Regression Seasonal ARIMA Generalized Autoregressive Conditional Heteroskedastic (Reg-SARIMA-GARCH) model (Sigauke and Chikobvu, 2011), exponential smoothing methods (Taylor, 2010, 2012), time series model for series exhibiting multiple complex seasonalities (TBATS) (Dang-Ha et al., 2017), regression models (Amber et al., 2015; Capozzoli et al., 2015; Kaytez et al., 2015), Support Vector Machine (SVM) models (Kaytez et al., 2015; Zhang et al., 2016; Jain et al., 2014), fuzzy models (Azadeh et al., 2010; Pereira et al., 2015), gray prediction models (Yao et al., 2003; Hamzacebi and Avni Es, 2014; Xu et al., 2017), and Kalman filters (Ghofrani et al., 2011b).

On the other hand, AI-based techniques are known to be generally adaptive and robust to non-stationary data and provide high accuracy, because the function is nonlinear and nonparametric. Many researchers have showed that neural network models are superior to classical models in terms of accuracy (Jovanović et al., 2015; Chae et al., 2016; Deb et al., 2016). However, there are several arguments for applying neural network models widely for any data, although AI-based techniques may be powerful. According to these studies, it is necessary to consider various techniques and select the best/relevant one, because AI-based techniques are not always adaptive, especially to linear data (Taskaya-Temizel and Casey, 2005).

Also, various studies of forecasting load demand in school buildings are widely conducted in recent studies. Lindberg et al. (2019) predicts aggregated hourly energy consumption in 114 non-residential buildings including school buildings by fitting regression models with outdoor temperature, time of day, and type of day as input values. Ribeiro et al. (2018) proposed a comparison results from using multiple machine learning methods to daily load demand in schools. Wang et al. (2019) applied long short-term memory (LSTM) networks, ANN, and SVR to predict multi-building energy use.

Although a lot of reviews for comparing conventional statistical models and AI-based methods are summarized in the past work (Daut et al., 2017; Li et al., 2019), it has not been conducted trying multiple relative time series forecasting methods and AI-based methods yet. The focus of this study is to examine the effectiveness of forecasting peak load demand for an institutional building using different statistical and artificial intelligence (AI)-based models under various scenarios. Section 3 introduces these models.

3. Models

The ARIMA, Reg-ARIMA, ARIMA-GARCH, Reg-ARIMA-GARCH, Holt-Winters' double seasonal exponential smoothing, Taylor's double seasonal exponential smoothing, TBATS, and neural network models are presented in this section.

3.1. The ARIMA model

The ARIMA model has undergone various developments over the years and used to be a benchmark model for time series analysis and forecasting (Box et al., 2008). Once the stationary assumption of the data is confirmed, various time series data are explained with different non-seasonal (p,q) orders and seasonal (P,Q) orders of ARIMA. When series $\{y_t | t = 1, 2, \dots, T\}$ follows ARIMA (p,d,q)(P,D,Q) with a mean of μ , the time series takes the form

$$\phi_p(l)\Phi_P(f)(1-l)^d(1-f)^D y_t = \theta_q(l)\Theta_Q(f)\varepsilon_t$$

where y_t represents the actual value of peak demand (in kilowatts) observed at time t ($t = 1, 2, \dots, T$) and ε_t represents the random errors assumed to be white noise during t , with a mean of zero and a constant variance of σ^2 . p , d , and q are integers and orders of the model. $\phi_p(l) = 1 - \phi_1 l - \dots - \phi_p l^p$, where p denotes the degree of the non-seasonal autoregressive polynomial. $\theta_q(l) = 1 - \theta_1 l - \dots - \theta_q l^q$, where q is the degree of the non-seasonal moving average polynomial. Moreover, for the seasonal operators, $\Phi_P(f) = 1 - \Phi_1 f - \dots - \Phi_P f^P$, where P denotes the degree of the seasonal autoregressive polynomial. $\Theta_Q(f) = 1 - \Theta_1 f - \dots - \Theta_Q f^Q$, where Q denotes the degree of the seasonal moving average polynomial. $(1-l)^d$ and $(1-f)^D$ are the non-seasonal and seasonal difference operators of order d and D respectively. s is a seasonal cycle.

3.2. The Reg-ARIMA model

Many factors affect electricity load demand, including holidays, temperature, and socio-economic variables. Typically, researchers regard climate-related variables as important factors imposing high demand on electronic appliances such as heating systems in winter and air-conditioning in summer. In this study, temperature, weekend and holiday indices are included as an explanatory variable in the Reg-ARIMA model.

The Reg-ARIMA model (Bell and Hillmer, 1983) is a regression ARIMA model with error terms. When the series $\{y_t | t = 1, 2, \dots, T\}$ follows the Reg-ARIMA model with k number of predictors, the time series takes the form

$$\phi_p(l)\Phi_P(f)(1-l)^d(1-f)^D \left(y_t - \sum_{i=1}^k \beta_i \chi_{ti} \right) = \theta_q(l)\Theta_Q(f)\varepsilon_t$$

where β_i is the coefficient of predictors χ_{ti} , and the other components are the same as those in ARIMA model.

3.3. The ARIMA-GARCH model

The ARIMA models can be specifically used when the assumption of constant variance. To adjust the fluctuations of the time series, Engle (Robert, 1982) proposed the autoregressive conditional heteroskedasticity (ARCH) model, and Bollerslev (1986) extended it as General ARCH (GARCH) model, whose main feature is that it can handle the data with heavier-tailed error distributions. The ARIMA-GARCH model is defined as

$$\phi_p(l)\Phi_P(f)(1-l)^d(1-f)^D y_t = c + \theta_q(l)\Theta_Q(f)\varepsilon_t$$

$$\varepsilon_t = z_t \sigma_t, \quad z_t \sim \text{i.i.d. with } E(z_t) = 0, \text{Var}(z_t) = 1$$

$$\sigma_t^2 = a_0 + \sum_{i=1}^q a_i \sigma_{t-i}^2 + \sum_{j=1}^p b_j \sigma_{t-j}^2$$

where y_t and polynomial components represent those as defined in Model 3.1. p is the order of GARCH process, q is the order of ARCH process. a_0 , a_i and b_j are constants, ε_t is the error term, σ_t^2 is the conditional variance of ε_t , z_t is a standardized error term.

3.4. The Reg-ARIMA-GARCH model

The Reg-ARIMA-GARCH model is a regression ARIMA model with error terms following a GARCH process. When the series $\{\psi_t | t = 1, 2, \dots, T\}$ follows the stationary Reg-ARIMA model with k number of predictors, and the model can be written as follows

$$\phi_p(l)\Phi_P(f)\psi_t = c + \theta_q(l)\Theta_Q(f)\varepsilon_t$$

$$\varepsilon_t = z_t \sigma_t, \quad z_t \sim \text{i.i.d. with } E(z_t) = 0, \text{Var}(z_t) = 1$$

$$\sigma_t^2 = \gamma \omega_t,$$

where

$$\gamma = (\alpha_0, \alpha_1, \dots, \alpha_q, \beta_1, \dots, \beta_p),$$

$$\omega_t = (1, \varepsilon_{t-1}^2, \dots, \varepsilon_{t-q}^2, \sigma_{t-1}^2, \dots, \sigma_{t-p}^2)$$

$$\psi_t = (1-l)^d(1-f)^D y_t - \sum_{i=1}^k \beta_i (1-l)^d(1-f)^D x_{ti}$$

where y_t is the original series before differencing, γ is a matrix of constants, ω_t is a matrix of error terms and conditional variance, β_i is the coefficient of predictors χ_{ti} , and the other components are the same as those in Reg-ARIMA model and ARIMA-GARCH model.

3.5. Holt–Winters' double seasonal exponential smoothing model

It is widely known that the exponential smoothing method (Winters, 1960) is simple to use and can be easily applied to time series data for the purposes of prediction. The advantage of this method is that it can be easily applied to seasonal patterns. Since the conventional Holt–Winters method was designed for a single seasonal cycle, the model has been extended to address multiple seasonal cycles. This model assumes that the process of white noise is correlated.

The traditional Holt–Winters method incorporates a single seasonal cycle as follows.

$$L_t = \alpha (y_t - S_{t-s}) + (1 - \alpha) (L_{t-1} + T_{t-1})$$

$$T_t = \beta (L_t - L_{t-1}) + (1 - \beta) T_{t-1}$$

$$S_t = \gamma (y_t - L_t) + (1 - \gamma) S_{t-s}$$

$$F_{t+h} = L_t + T_t \times h + S_{t+h-s}$$

where y_t represents the actual value of peak demand, S_t represents the seasonal component observed over time t ($t = 1, 2, \dots, T$), and s is the seasonal cycle. The components L_t and T_t are the level and trend components of the series at time t , respectively. The coefficients α, β, γ are smoothing parameters. F_{t+h} is the predicting value of h ahead from time t .

The Holt–Winters' double seasonal method can be written as below.

$$L_t = \alpha (y_t - S_{t-s_1} - D_{t-s_2}) + (1 - \alpha) (L_{t-1} + T_{t-1})$$

$$T_t = \beta (L_t - L_{t-1}) + (1 - \beta) T_{t-1}$$

$$S_t = \gamma (y_t - L_t - D_{t-s_2}) + (1 - \gamma) S_{t-s_1}$$

$$D_t = \delta (y_t - L_t - S_{t-s_1}) + (1 - \delta) D_{t-s_2}$$

$$F_{t+h} = L_t + T_t \times h + S_{t+h-s_1} + D_{t+h-s_2}$$

where s_1, s_2 are double seasonal cycles, and S_t, D_t are seasonal components. The initial values are calculated as follows.

$$L_{s_1} = \frac{1}{s_1} \sum_{t=1}^{s_1} y_t, L_{s_2} = \frac{1}{s_2} \sum_{t=1}^{s_2} y_t$$

$$T_{s_1} = \frac{1}{s_1^2} \left(\sum_{t=s_1+1}^{2s_1} y_t - \sum_{t=1}^{s_1} y_t \right), T_{s_2} = \frac{1}{s_2^2} \left(\sum_{t=s_2+1}^{2s_2} y_t - \sum_{t=1}^{s_2} y_t \right)$$

$$S_1 = y_1 - L_{s_1}, \dots, S_{s_1} = y_{s_1} - L_{s_1}$$

$$D_1 = y_1 - L_{s_2}, \dots, D_{s_2} = y_{s_2} - L_{s_2}$$

3.6. Taylor's double seasonal exponential smoothing model

Taylor (2010) introduced the extended version of Holt–Winters double seasonal method to address multiple seasonality. This model also assumes that the process of white noise is correlated. The F_{t+h} formula is expressed as follows

$$F_{t+h} = L_t + T_t \times h + S_{t+h-s_1} + D_{t+h-s_2} + \phi^h [y_t - L_{t-1} - T_{t-1} - S_{t-s_1} - D_{t-s_2}]$$

where ϕ represents the adjusted first-order coefficient, and the smoothing parameters are given by $\alpha, \beta, \gamma, \delta$, and ϕ . Moreover, s_1, s_2 are double seasonal cycles.

3.7. The TBATS model

TBATS refers to Trigonometrical transformation, Box–Cox transformation (Box and Cox, 1964), ARMA errors, and Trends and Seasonal components. De Livera et al. (2011) proposed modified state space models for exponential smoothing to avoid

problems related to a wider seasonal pattern variety and to handle correlated errors. With regard to the nonlinearity issue, the model is restricted to linear homoscedasticity, but the Box–Cox transformation (Box and Cox, 1964) is used for some types of non-linearity. This class of model is named BATS (Box–Cox transformation, ARMA errors, Trend and Seasonal components) and is defined as follows.

$$y_t^{(\omega)} = \begin{cases} \frac{y_t^\omega - 1}{\omega}, & \omega \neq 0 \\ \log(y_t), & \omega = 0 \end{cases}$$

$$y_t^{(\omega)} = l_{t-1} + \phi b_{t-1} + \sum_{i=1}^T S_{t-m_i}^{(i)} + d_t$$

$$l_t = l_{t-1} + \phi b_{t-1} + \alpha d_t$$

$$b_t = (1 - \phi) b + \phi b_{t-1} + \beta d_t$$

$$S_t^{(i)} = S_{t-m_i}^{(i)} + \gamma_i d_t$$

$$d_t = \sum_{i=1}^p \varphi_i d_{t-i} + \sum_{i=1}^q \theta_i \varepsilon_{t-i} + \varepsilon_t$$

where $y_t^{(\omega)}$ is the Box–Cox transformed observation for parameter ω at time t . l_t represents the local level data, b is the long-term trend, and b_t is the short-term trend within time period t . Rather than converging on zero, the value of b_t finally converges on b . ϕ is a damping parameter for the trend. d_t is a series of ARMA models with orders (p, q) and ε_t is the white noise process with a mean of zero and a constant variance of σ^2 . m_i is the i th seasonal cycle. α, β , and γ_i are the smoothing parameters for $i = 1, \dots, T$.

To accommodate non-integer seasonality, the trigonometric seasonal approach is incorporated into the model so that the estimation time (which increases with the number of parameters) can be reduced. The final TBATS model with arguments $(\omega, \phi, p, q, \{m_1, k_1\}, \{m_2, k_2\}, \dots, \{m_T, k_T\})$ is explained with some additional equations as seen below.

$$S_t^{(i)} = \sum_{j=1}^{k_i} S_{j,t}^{(i)}$$

$$S_{j,t}^{(i)} = S_{j,t-1}^{(i)} \cos \lambda_j^{(i)} + S_{j,t-1}^{*(i)} \sin \lambda_j^{(i)} + \gamma_1^{(i)} d_t$$

$$S_{j,t}^{*(i)} = -S_{j,t-1}^{(i)} \sin \lambda_j^{(i)} + S_{j,t-1}^{(i)} \cos \lambda_j^{(i)} + \gamma_2^{(i)} d_t$$

where k_i is the number of harmonics for $S_t^{(i)}$, which is a seasonal component. $\gamma_1^{(i)}$ and $\gamma_2^{(i)}$ are the smoothing parameters and $\lambda_j^{(i)} = \frac{2\pi j}{m_i} \cdot S_{j,t}^{(i)}$ is the stochastic level of the i th seasonal component by $S_{j,t}^{(i)}$, and $S_{j,t}^{*(i)}$ is stochastic growth of the i th seasonal component.

3.8. Artificial neural network model

ANN models are forecasting methods introduced by McCulloch and Pitts (1943), based on an algorithm of threshold logic. They are most widely used in machine learning models. The basic concept of these models is similar to manner in which the human brain works. The brain consists of neurons that link data processing and recollection processing, and these neurons are connected by synaptic weights. ANN models are estimated by calculating the weights as training inputs and outputs from past records. Therefore, they are advantageous in that they can explain nonlinear relationships between inputs and outputs. The nonlinear autoregressive network with exogenous inputs (NARX) is the ANN-based model with additional input variables. Fig. 1 shows the structure of ANN model.

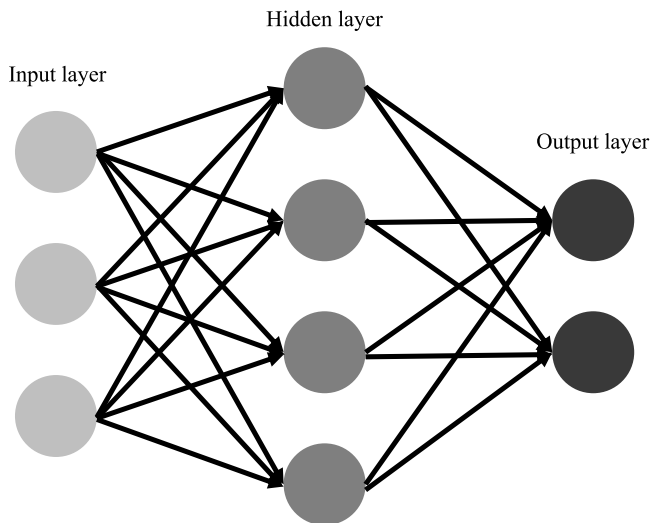


Fig. 1. Artificial neural network structure.

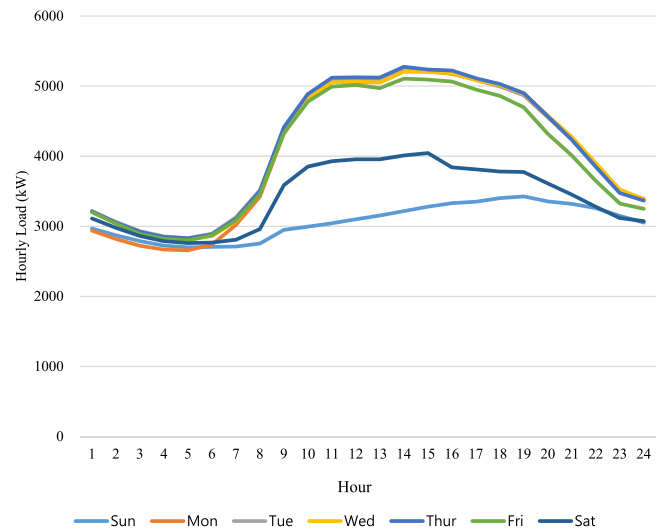


Fig. 3. Average daily load demand plot.

4. Data

The data considered in this paper were obtained from Chung-ang University, Seoul, Korea. They were collected at every 1-h interval during the period from January 1st to December 31th, 2017. The total number of data points collected over 1 year is 8760.

Institutional buildings may be considered as being similar to commercial buildings, but the former can take on complex forms consisting of classrooms, administrative offices, and dormitories. Therefore, in order to understand the demand pattern of the students, calendar effects such as weekends and public holidays should be reflected in the model as factors. Moreover, temperature was considered as a factor because the circumstances related to the weather are highly related to users' behavior with regard to the use of air-conditioning or heating appliances. Some studies have suggested deriving considering heating and cooling degree days (HDD and CDD, respectively) instead of temperature (Jung and Kim, 2014). Since the data covers a year, HDD and CDD indices can provide more accurate relationship between people's behaviors and the amount of energy consumption. Also, to accomplish the main object of this study to compare the various models for the STLF, we decided to use real-time hourly weather information from Korea Meteorological Administration as predictor values in Reg-ARIMA models and NARX model. The HDD and CDD formulas shown as below.

$$\text{HDD} = \begin{cases} 18 - T_t, & \text{if } T_t \leq 18 \\ 0, & \text{else} \end{cases}$$

$$\text{CDD} = \begin{cases} T_t - 24, & \text{if } T_t \geq 24 \\ 0, & \text{else} \end{cases}$$

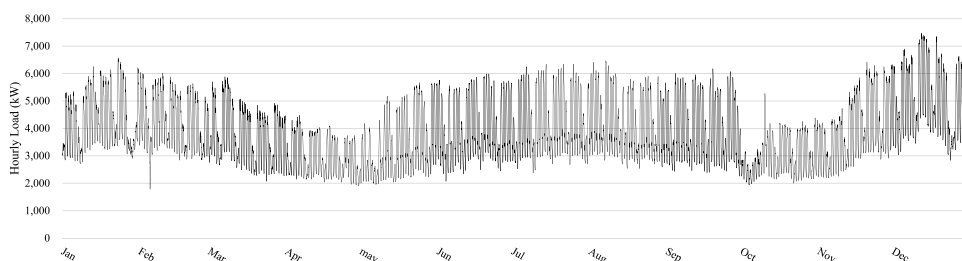


Fig. 2. Hourly load demand plot.

Fig. 2 shows a general time series profile of the demand data. The demand shows clear patterns of daily and weekly seasonality. Fig. 3 plots the average daily demand by hour, and it can be seen higher demand occurs on weekdays, and lower demand, on weekends. Monday through Friday were grouped into weekdays, and the others into weekends in a weekend dummy variable. Also, we can see a higher fluctuation of the demand in summer and winter seasons, while demands in spring and fall seasons fluctuate lower. During national holiday seasons in January and October, there is a continuous decline pattern going on for a week.

Fig. 4 shows the temperature profile and data obtained from Korea Meteorological Administration website. Daily seasonal effects can be observed, and temperature is the hottest in summer and the coldest in winter. There are two reference lines for converting temperature to HDD and CDD at 18 °C and 24 °C, respectively. Fig. 5 shows a scatter plot, which indicates a quadratic relationship between peak load demand and temperature. It provides a background for converting temperature into two new indicators (HDD, CDD).

5. Application of the models

The peak load demand data considered in this study comprise a total of 8760 observations over 1 year. They are fitted to the models described in Section 3. Then, 7296 observations made over a period of 10 months are used for the training, and the rest for the validation set. In this study, an automatic model selection approach for optimizing each model is considered to help identify the optimal model in a real-life situation such as the one presented here. The moving window is a calculation that

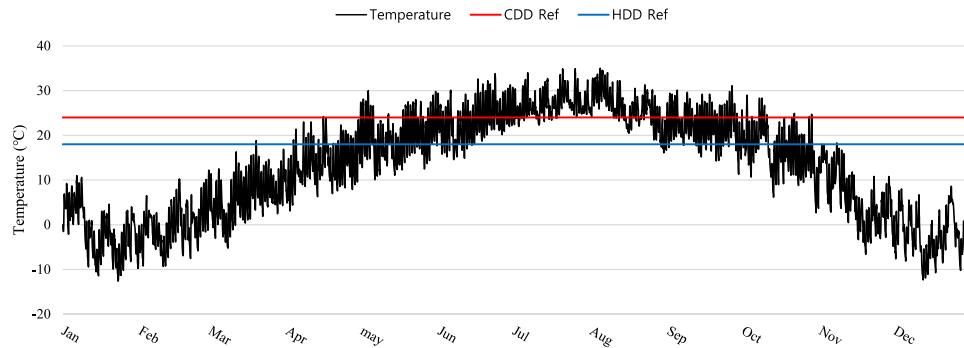


Fig. 4. Hourly temperature plot.

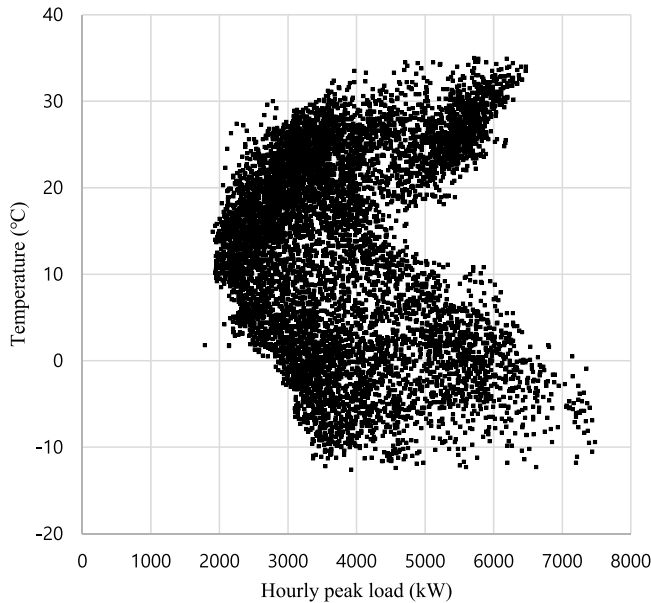


Fig. 5. Load-temperature scatterplot.

uses the fixed period of the training set, and the parameters of the models are estimated at each step using the minimum Akaike Information Criterion (AIC). Since the model estimations are updated at each k step, we obtain k number of different results for a single model.

The best-fit models were chosen according to the minimum AIC, and the identification of best ARIMA models and Reg-ARIMA models is demonstrated in Tables 1–2. The Ljung–Box Q-statistics from the ARIMA model ($p = 0.3558$) and Reg-ARIMA model ($p = 0.921$) on standardized residuals carried out insignificant indicating that there is no autocorrelation left. However, the Ljung–Box Q-statistics from the ARIMA model ($p < 0.0001$) and Reg-ARIMA model ($p < 0.0001$) on squared standardized residuals showed significant indicating that there is heteroskedasticity. The Engle's LM tests were conducted, and it proved that there is GARCH effects in the model. We expanded the ARIMA model and Reg-ARIMA model by fitting volatility with GARCH model.

Tables 3–9 show the parameters estimated in the training set. Table 4 represents all the coefficients of the dummy variables that the peak demand decreases on weekends and holidays, on the other hand, it increases when the temperature is above 24 °C or below 18 °C. It proves that the use of air-conditioners and heating appliances have impact on the demand rising. For the ANN model, 38 non-seasonal input neurons and 1 seasonal input neuron with 20 nodes in the hidden layer were generated and represented as

Table 1
Identification of best ARIMA models.

| $(p, d, q, P, D, Q)_{s=24}$ | AIC |
|-----------------------------|----------------|
| (1,0,1,1,1,1) | 90780.6 |
| (1,0,1,0,1,1) | 90962.4 |
| (3,0,2,2,1,0) | 91280.7 |
| (1,0,2,2,1,0) | 91545.3 |
| (3,0,1,0,1,0) | 92804.5 |

Table 2
Identification of best Reg-ARIMA models.

| $(p, d, q, P, D, Q)_{s=24}$ | AIC |
|-----------------------------|----------------|
| (1,0,1,1,1,1) | 90719.4 |
| (1,0,1,0,1,1) | 90902.6 |
| (3,0,2,2,1,0) | 91215.7 |
| (2,0,2,2,1,0) | 91222.7 |
| (1,0,2,2,1,0) | 91504.3 |

Table 3
Parameter estimations of the ARIMA (1, 0, 1) (1, 1, 1)_{s=24} model.

| Parameter | Estimate (S.E.) |
|------------|------------------|
| ϕ_1 | 0.9634 (0.0032) |
| θ_1 | 0.3226 (0.0093) |
| Φ_1 | 0.1798 (0.0133) |
| Θ_1 | −0.8993 (0.0056) |

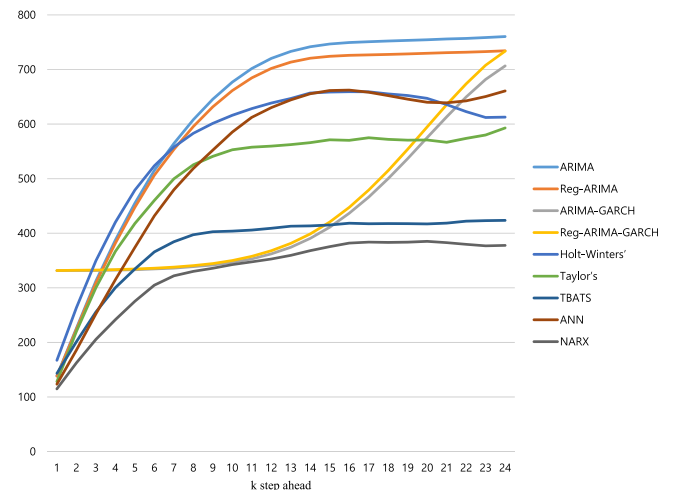


Fig. 6. Forecast performance evaluations in terms of RMSE.

(38-1-20) with daily seasonality ($s = 24$). For the ANN model with external variables of weekends, HDD, CDD and holidays, one more hidden layer was used, and it is represented as (38-1-22) with daily seasonality.

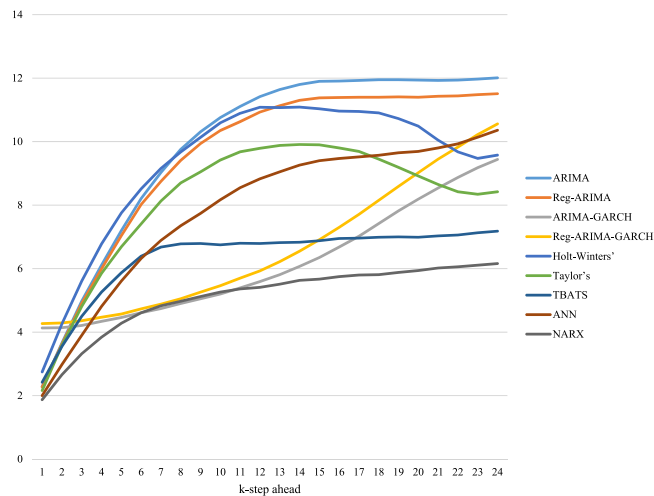


Fig. 7. Forecast performance evaluations in terms of MAPE.

Table 5

Parameter estimations of the $ARIMA(2, 0, 3)(0, 1, 0)_{s=24} - GARCH(1, 1)$ model.

| Parameter | Estimate |
|------------|-----------|
| c | -25.3066 |
| ϕ_1 | 1.6808 |
| ϕ_2 | -0.7149 |
| θ_1 | -1.5059 |
| θ_2 | 0.5571 |
| θ_3 | -0.0513 |
| a_0 | 1316.4546 |
| a_1 | 0.1285 |
| b_1 | 0.8200 |

6. Performance evaluations

In this section, the models presented in this work are compared by using root-mean-square error (RMSE) and mean absolute percentage error (MAPE). These methods are generally used in short-term load forecasting to present error.

The RMSE is defined as

$$RMSE = \sqrt{\frac{1}{n} \sum_{t=1}^n (\hat{y}_t - y_t)^2}$$

where y_t is the actual value and \hat{y}_t is the forecasted demand at time t , respectively. Also, the equation of mean absolute percentage error (MAPE) is given by

$$MAPE = \frac{100}{n} \sum_{t=1}^n \left| \frac{y_t - \hat{y}_t}{y_t} \right|$$

where the explanation of the components matches that of formula of RMSE.

Table 4

Parameter estimations of the $Reg - ARIMA(1, 0, 1)(1, 0, 1)_{s=24}$ model.

| Parameter | Estimate |
|-------------------|----------|
| ϕ_1 | 0.9611 |
| θ_1 | 0.3201 |
| Φ_1 | 0.1805 |
| Θ_1 | -0.9022 |
| $\beta_{weekend}$ | -41.2886 |
| $\beta_{holiday}$ | -22.9817 |
| β_{CDD} | 19.1334 |
| β_{HDD} | 22.5082 |

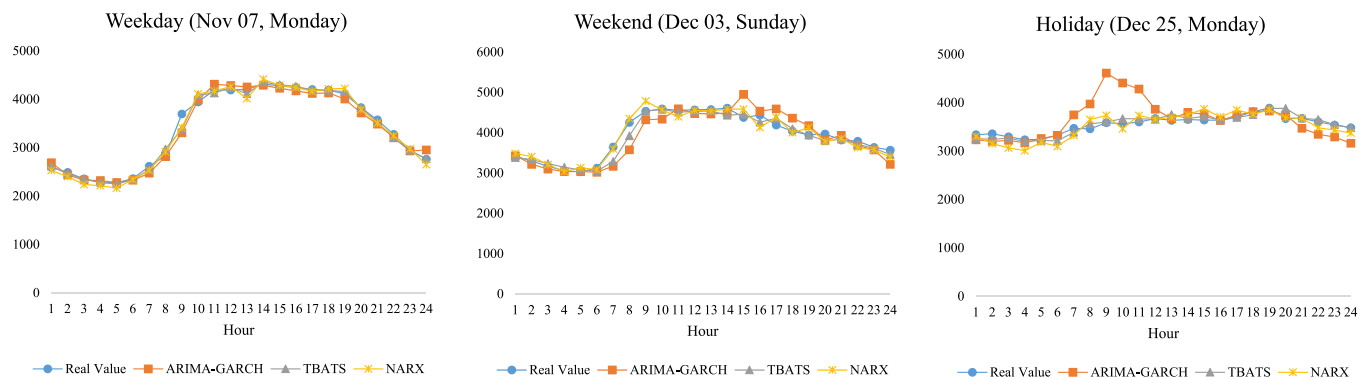


Fig. 8. Graphical plots of 1 step-ahead forecasting results.

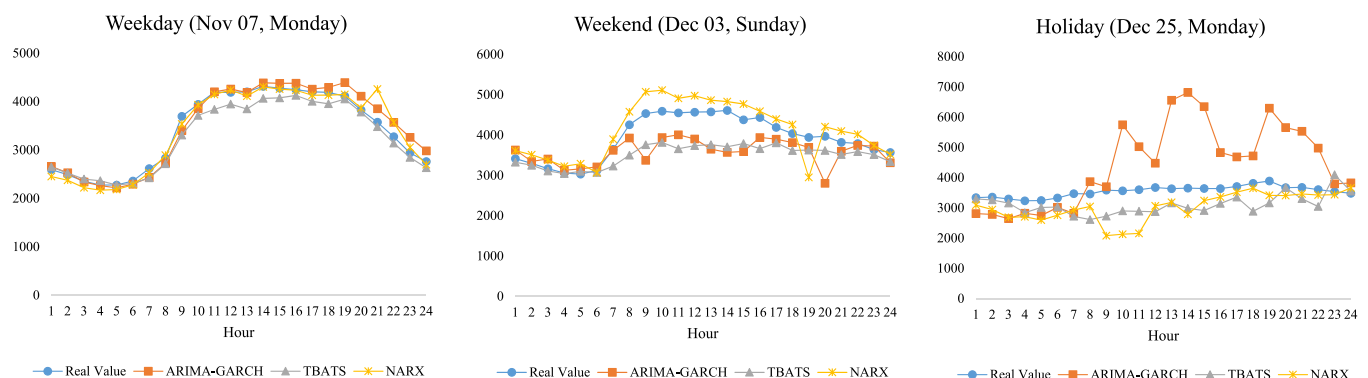


Fig. 9. Graphical plots of 24 step-ahead forecasting results.

Table 10 presents the results of accuracy tests in the fixed period of training set from January 1st to October 31th, 2017. It showed that the ANN model with external variables (NARX) present the lowest RMSE and MAPE.

The RMSEs and MAPEs of k step-ahead forecasts in out of sample period from November 1st to December 31th 2017 are presented in Tables 11 and 12, respectively. Each step shows k step-ahead performances in every hour for 24 steps. Table 11 shows that the NARX model present the lowest RMSE through the whole steps. Table 12 provides a comparison of the models with regard to the MAPE for k step-ahead forecasting. Here, the NARX model shows the best performance, except for steps 7–10, whereas the ARIMA-GARCH model shows slightly higher prediction accuracy.

Figs. 6 and 7 show graphical plots for Tables 11 and 12. In general, the performances of the models in 1 step ahead forecasting show similar patterns to the training set. GARCH-based models stay stable until 9 step-ahead although the models produced lower accurate results in 1 step-ahead, while the accuracies of the other models diminish rapidly. However, the RMSEs and MAPEs of the GARCH-based models increase exponentially through the steps. Meanwhile, the other models result in robust after 9 step-ahead forecasting.

Let us take a close look at each model. The Reg-ARIMA model provides slightly better accuracy than the ARIMA model, despite the significant coefficients of the external variables. Plus, against expectations, it is shown that it is not helpful using the inputs in the ARIMA-GARCH models. By contrast, the NARX model provides much higher accuracy than the ANN model, that is, the external variables work well in ANN model better than the ARIMA model. Similar to various other studies that proved weather and holiday effects in forecasting, our work showed that applying accurate external variables to the model is crucial for electricity demand forecasting with the ANN model. However, it is demonstrated that using exogenous variables would not universally help in forecasting accuracy improvement even though the real-time values are used as inputs. It is advisable to check if it is beneficial adding extra input datasets because sometimes this task might lead to be complex and time consuming but not as good as we expect the results to be.

We also compare three smoothing methods. The results indicate that using the TBATS model can provide the best fit, and the Holt–Winters' model show lower accuracy than TBATS or Taylor's model. It indicates that adjusting the autoregressive smoothing parameter ϕ in Taylor's models leads to a better performance than Holt–Winters' model. In 1 step-ahead forecasting, the Taylor's models are superior to the TBATS models. However, outperformance of the TBATS model may indicates that (1) the assumption that the error terms that are distributed white noise process not be met. (2) the Box–Cox transformation worked well with the nonlinearity of the series. Using the TBATS model is worth considering in case that extra input datasets are not available.

Figs. 8 and 9 are comparison plots of actual values and predicted values on a randomly selected weekday, weekend and Christmas from three representing outperformed models (ARIMA-GARCH, TBATS, NARX models) in 1 step-ahead and 24 step-ahead, respectively. Fig. 8 indicates that three models have good results in on weekday, but high fluctuated predicted values estimated from ARIMA-GARCH model on weekend and holiday. In Fig. 9, also well fitted lines are shown on weekday from all models, however, the ARIMA-GARCH model tends to underestimate or overestimate the values on weekend and holiday. The graphs show that the NARX model and TBATS model can provide a good fit in general. To sum up the whole results above, we find that the NARX model gives the lowest error and shows robustness in view of both RMSE and MAPE.

Table 6

Parameter estimations of the Reg – ARIMA (4, 0, 2) (0, 1, 0)_{s=24} – GARCH(1, 1) model.

| Parameter | Estimate |
|-------------------|-----------|
| c | −25.3069 |
| ϕ_1 | 1.2150 |
| ϕ_2 | −1.0280 |
| ϕ_3 | 0.1195 |
| ϕ_4 | 0.1451 |
| θ_1 | −0.9864 |
| θ_2 | 0.9887 |
| $\beta_{weekend}$ | −1.6578 |
| $\beta_{holiday}$ | 55.3015 |
| β_{CDD} | 6.9378 |
| β_{HDD} | 1.5125 |
| a_0 | 1174.1081 |
| a_1 | 0.1027 |
| b_1 | 0.8480 |

Table 7

Parameter estimations of the Holt–Winters double seasonal exponential smoothing model.

| Parameter | Estimate |
|-----------------------|----------|
| α (level) | 0.8323 |
| β (trend) | 0.0001 |
| γ (seasonal 1) | 0.9900 |
| δ (seasonal 2) | 0.3494 |

Table 8

Parameter estimations of Taylor's adjusted double seasonal exponential smoothing model.

| Parameter | Estimate |
|-----------------------|----------|
| α (level) | 0.5987 |
| β (trend) | 0.0059 |
| γ (seasonal 1) | 0.2625 |
| δ (seasonal 2) | 0.3804 |
| ϕ | 0.4463 |

Table 9

Parameter estimations of the TBATS model.

| Parameter | Estimate |
|------------------|----------|
| ω | 0.3804 |
| α | 0.5987 |
| β | 0.0059 |
| γ | 0.2625 |
| ϕ | 0.4463 |
| $\gamma_1^{(1)}$ | 0.0007 |
| $\gamma_1^{(2)}$ | <0.0001 |
| $\gamma_2^{(1)}$ | −0.0009 |
| $\gamma_2^{(2)}$ | 0.0006 |
| φ_1 | 1.0850 |
| φ_2 | 0.3670 |
| φ_3 | −0.5620 |
| θ_1 | −0.2341 |
| θ_2 | −0.5023 |
| θ_3 | 0.1252 |
| θ_4 | −0.1114 |
| θ_5 | −0.0031 |

7. Conclusion

Accurate energy demand forecasting is a very important issue for decision makers and power generation companies in terms of policy creation and power generation planning, respectively. Thus, many attempts have been made to improve the performance of peak load forecasting. This paper adds to the literature in this area by investigating relevant time series and AI models for 1-h interval peak load demand forecasting in an institutional building in Seoul, Korea.

Table 10

Forecast performance evaluations in training set.

| Models | RMSE | MAPE |
|-----------------|--------------|-------------|
| ARIMA | 123.73 | 2.44 |
| Reg-ARIMA | 123.14 | 2.43 |
| ARIMA-GARCH | 146.76 | 2.72 |
| Reg-ARIMA-GARCH | 147.25 | 2.83 |
| Holt-Winters' | 115.86 | 2.37 |
| Taylor's | 105.16 | 2.11 |
| TBATS | 134.43 | 2.67 |
| ANN | 92.82 | 1.85 |
| NARX | 85.44 | 1.69 |

ARIMA models, GARCH-based models, multiple seasonal exponential smoothing methods, and ANN models were used and validated to achieve this objective. The results showed that the ANN model with external variables (NARX) demonstrates the

best prediction accuracy and provides robust and stable results compared to other traditional time series models.

Many past works have shown that using HDD, CDD and holiday variables is crucial to predict peak load demand. In this study, the NARX model provided the lowest MAPE from 1-h ($k = 1$) to 1-d ($k = 24$) ahead forecasting. This proves that the weather and holiday features play a considerable role in load demand in the studied institutional building. However, the ARIMA model with external variables did not show high accuracy for lead times from 1-h to 1-d ahead forecasting. Nonetheless, the coefficients of the external variables offer some insights into which factor might have influenced load demand more. We believe that as external variables were added to the ARIMA model, the complexity of the model increased, leading to over-fitting problems. Also, even though the ARIMA-GARCH model was the best fitted model for the period of 7 to 10-h ahead forecasting, it tends to estimate too much volatility in weekend and holidays. Contrary to other results from the Reg-ARIMA models and NARX models,

Table 11

Forecast performance evaluations in terms of RMSE.

| k | ARIMA | Reg-ARIMA | ARIMA-GARCH | Reg-ARIMA-GARCH | Holt-Winters' | Taylor's | TBATS | ANN | NARX |
|-----|--------|-----------|-------------|-----------------|---------------|----------|--------|--------|---------------|
| 1 | 138.69 | 138.11 | 331.56 | 331.68 | 167.37 | 128.29 | 143.51 | 123.49 | 114.93 |
| 2 | 226.12 | 224.15 | 331.79 | 332.20 | 263.69 | 220.20 | 201.39 | 185.98 | 162.61 |
| 3 | 312.75 | 308.98 | 331.84 | 332.60 | 349.69 | 300.19 | 255.91 | 252.52 | 205.55 |
| 4 | 387.50 | 381.93 | 332.58 | 333.33 | 420.35 | 366.90 | 300.28 | 315.03 | 241.67 |
| 5 | 454.93 | 447.60 | 333.25 | 334.56 | 479.18 | 417.78 | 334.60 | 374.03 | 275.44 |
| 6 | 515.28 | 506.28 | 334.75 | 335.95 | 523.59 | 460.22 | 365.82 | 431.79 | 304.84 |
| 7 | 564.40 | 553.53 | 336.22 | 337.92 | 557.77 | 499.69 | 384.49 | 479.55 | 321.96 |
| 8 | 607.99 | 595.49 | 338.71 | 340.73 | 583.11 | 525.48 | 397.37 | 518.71 | 330.10 |
| 9 | 645.69 | 631.64 | 341.77 | 344.54 | 601.33 | 540.88 | 402.80 | 552.25 | 335.82 |
| 10 | 677.01 | 661.26 | 346.63 | 350.02 | 616.26 | 553.01 | 403.76 | 585.46 | 342.53 |
| 11 | 701.95 | 684.63 | 353.01 | 357.70 | 628.42 | 557.69 | 405.83 | 612.40 | 347.66 |
| 12 | 720.33 | 701.84 | 362.32 | 367.94 | 638.56 | 559.58 | 409.10 | 630.15 | 352.84 |
| 13 | 733.24 | 713.56 | 374.37 | 381.38 | 646.86 | 562.48 | 412.99 | 644.31 | 359.50 |
| 14 | 741.68 | 720.58 | 390.63 | 398.73 | 656.91 | 565.99 | 413.38 | 655.62 | 368.11 |
| 15 | 746.70 | 724.32 | 411.03 | 420.61 | 658.71 | 571.15 | 415.00 | 661.48 | 375.44 |
| 16 | 749.43 | 726.06 | 436.58 | 447.35 | 659.40 | 570.30 | 418.27 | 662.33 | 381.98 |
| 17 | 750.94 | 726.83 | 466.20 | 479.05 | 659.21 | 575.02 | 417.39 | 658.47 | 383.81 |
| 18 | 752.20 | 727.68 | 500.17 | 514.89 | 655.25 | 571.99 | 417.63 | 652.16 | 383.09 |
| 19 | 753.35 | 728.65 | 536.62 | 553.90 | 652.36 | 570.52 | 417.57 | 645.65 | 383.69 |
| 20 | 754.59 | 729.73 | 575.20 | 594.83 | 647.20 | 570.84 | 417.02 | 640.05 | 385.21 |
| 21 | 755.98 | 730.86 | 613.21 | 635.52 | 635.67 | 566.70 | 418.47 | 639.05 | 382.86 |
| 22 | 757.03 | 731.73 | 649.77 | 673.78 | 622.94 | 573.79 | 422.04 | 642.62 | 379.70 |
| 23 | 758.55 | 732.91 | 681.79 | 707.82 | 612.09 | 579.96 | 423.12 | 650.39 | 376.97 |
| 24 | 760.42 | 734.30 | 706.55 | 733.57 | 612.81 | 592.87 | 423.53 | 660.69 | 377.74 |

Table 12

Forecast performance evaluations in terms of MAPE.

| k | ARIMA | Reg-ARIMA | ARIMA-GARCH | Reg-ARIMA-GARCH | Holt-Winters' | Taylor's | TBATS | ANN | NARX |
|-----|-------|-----------|-------------|-----------------|---------------|----------|-------|-------|-------------|
| 1 | 2.28 | 2.27 | 4.13 | 4.27 | 2.75 | 2.16 | 2.42 | 2.00 | 1.87 |
| 2 | 3.66 | 3.63 | 4.14 | 4.29 | 4.26 | 3.59 | 3.55 | 2.98 | 2.66 |
| 3 | 4.98 | 4.91 | 4.21 | 4.36 | 5.61 | 4.81 | 4.50 | 3.90 | 3.32 |
| 4 | 6.11 | 5.99 | 4.34 | 4.47 | 6.78 | 5.85 | 5.26 | 4.81 | 3.84 |
| 5 | 7.20 | 7.04 | 4.46 | 4.57 | 7.76 | 6.69 | 5.87 | 5.61 | 4.28 |
| 6 | 8.21 | 8.02 | 4.61 | 4.73 | 8.51 | 7.41 | 6.39 | 6.32 | 4.61 |
| 7 | 9.03 | 8.75 | 4.74 | 4.88 | 9.16 | 8.13 | 6.68 | 6.89 | 4.83 |
| 8 | 9.76 | 9.41 | 4.90 | 5.05 | 9.67 | 8.70 | 6.78 | 7.35 | 4.97 |
| 9 | 10.31 | 9.94 | 5.05 | 5.26 | 10.14 | 9.05 | 6.79 | 7.74 | 5.12 |
| 10 | 10.76 | 10.35 | 5.20 | 5.46 | 10.59 | 9.42 | 6.75 | 8.17 | 5.26 |
| 11 | 11.11 | 10.63 | 5.39 | 5.70 | 10.89 | 9.68 | 6.80 | 8.55 | 5.36 |
| 12 | 11.42 | 10.93 | 5.59 | 5.93 | 11.08 | 9.79 | 6.79 | 8.83 | 5.41 |
| 13 | 11.64 | 11.13 | 5.81 | 6.22 | 11.07 | 9.88 | 6.82 | 9.05 | 5.51 |
| 14 | 11.80 | 11.30 | 6.07 | 6.55 | 11.09 | 9.91 | 6.83 | 9.26 | 5.63 |
| 15 | 11.90 | 11.38 | 6.35 | 6.91 | 11.03 | 9.90 | 6.88 | 9.40 | 5.67 |
| 16 | 11.91 | 11.39 | 6.68 | 7.30 | 10.96 | 9.80 | 6.95 | 9.47 | 5.75 |
| 17 | 11.93 | 11.40 | 7.02 | 7.71 | 10.95 | 9.69 | 6.96 | 9.52 | 5.80 |
| 18 | 11.95 | 11.40 | 7.42 | 8.15 | 10.91 | 9.45 | 6.99 | 9.57 | 5.81 |
| 19 | 11.95 | 11.41 | 7.82 | 8.59 | 10.72 | 9.19 | 7.00 | 9.65 | 5.88 |
| 20 | 11.94 | 11.40 | 8.19 | 9.02 | 10.49 | 8.92 | 6.99 | 9.69 | 5.94 |
| 21 | 11.93 | 11.43 | 8.54 | 9.45 | 10.05 | 8.65 | 7.03 | 9.80 | 6.02 |
| 22 | 11.94 | 11.44 | 8.87 | 9.83 | 9.68 | 8.42 | 7.06 | 9.93 | 6.06 |
| 23 | 11.97 | 11.48 | 9.18 | 10.22 | 9.47 | 8.34 | 7.13 | 10.14 | 6.11 |
| 24 | 12.01 | 11.51 | 9.44 | 10.56 | 9.58 | 8.42 | 7.18 | 10.36 | 6.16 |

it is demonstrated that the exogenous variables did not improve forecasting accuracy in the ARIMA-GARCH models. Therefore, it is a point to be considered that whether the external variables are helpful factors and if so, balancing the trade-off between accuracy and model simplicity.

In this study, we mainly focus on comparing performances of the ARIMA-based models, exponential smoothing methods, and AI-based models. However, different adaptations of the models, such as SVM models, fuzzy models, gray prediction models, and Kalman Filters will be discussed in the future study, because those models and issues can be interesting papers to be analyzed.

Future studies should focus on fitting the same models using data from different institutional buildings, the goal being to build an optimal, customized model for each single unit/building according to building size, construction years and types of external wall. Moreover, the same trial will be conducted with daily peak load demand with other relevant variables such as the amount of internet traffic and the number of students from the entry log from electronic records systems.

Demand-side management has replaced the top-down policy in the world energy market. The next generation of energy policies thus needs to track and plan for load demand of relatively small areas as well. The data we presented in this study had strong seasonal patterns because of the characteristics of the institution's routine. In order to increase the scientific validity of our results, the same procedure will be applied to other (i.e., non-institutional) organizations' peak load data in future studies.

Declaration of competing interest

The authors declare that they have no known competing financial interests or personal relationships that could have appeared to influence the work reported in this paper.

Acknowledgment

This research is supported by the National Research Foundation of Korea (Grant No. 2016R1D1A1B01014954).

References

- Amber, K.P., Aslam, M.W., Hussain, S.K., 2015. Electricity consumption forecasting models for administration buildings of the UK higher education sector. *Energy Build.* 90, 127–136.
- Amjadi, Nima, 2001. Short-term hourly load forecasting using time-series modeling with peak load estimation capability. *IEEE Trans. Power Syst.* 16 (3), 498–505.
- Azadeh, A., Saberi, M., Seraj, O., 2010. An integrated fuzzy regression algorithm for energy consumption estimation with non-stationary data: a case study of Iran. *Energy* 35 (6), 2351–2366.
- Bell, William R., Hillmer, Steven C., 1983. Modeling time series with calendar variation. *J. Am. Stat. Assoc.* 78 (383), 526–534.
- Bollerslev, Tim, 1986. Generalized autoregressive conditional heteroskedasticity. *J. Econometrics* 31 (3), 307–327.
- Borojeni, Kianoosh G., et al., 2017. A novel multi-time-scale modeling for electric power demand forecasting: From short-term to medium-term horizon. *Electr. Power Syst. Res.* 142, 58–73.
- Box, George E.P., Cox, David R., 1964. An analysis of transformations. *J. R. Stat. Soc. Ser. B Stat. Methodol.* 26 (2), 211–243.
- Box, George E.P., Jenkins, Gwilym M., Reinsel, Gregory C., 2008. *Forecasting. Time Ser. Anal.* 137–191.
- Capozzoli, Alfonso, Grassi, Daniele, Causone, Francesco, 2015. Estimation models of heating energy consumption in schools for local authorities planning. *Energy Build.* 105, 302–313.
- Chae, Young Tae, et al., 2016. Artificial neural network model for forecasting sub-hourly electricity usage in commercial buildings. *Energy Build.* 111, 184–194.
- Dahl, Magnus, et al., 2018. Improving short-term heat load forecasts with calendar and holiday data. *Energies* 11 (7), 1678.
- Dang-Ha, The-Hien, Bianchi, Filippo Maria, Olsson, Roland, 2017. Local short term electricity load forecasting: Automatic approaches. In: 2017 International Joint Conference on Neural Networks (IJCNN). IEEE.
- Daut, Mohammad Azhar Mat, et al., 2017. Building electrical energy consumption forecasting analysis using conventional and artificial intelligence methods: A review. *Renew. Sustain. Energy Rev.* 70, 1108–1118.
- De Livera, Alysha M., Hyndman, Rob J., Snyder, Ralph D., 2011. Forecasting time series with complex seasonal patterns using exponential smoothing. *J. Amer. Statist. Assoc.* 106 (496), 1513–1527.
- Deb, Chirag, et al., 2016. Forecasting diurnal cooling energy load for institutional buildings using Artificial Neural Networks. *Energy Build.* 121, 284–297.
- Dehghanzadeh, Ahmad, et al., 2018. Mid-term load forecasting for Iran power system using seasonal autoregressive integrated moving average model (SARIMA). In: *Electrical Engineering (ICEE), Iranian Conference On.* IEEE.
- Ekonomou, L., 2010. Greek long-term energy consumption prediction using artificial neural networks. *Energy* 35 (2), 512–517.
- Fan, H., MacGill, I.F., Sproul, A.B., 2017. Statistical analysis of drivers of residential peak electricity demand. *Energy Build.* 141, 205–217.
- Ghedamsi, R  bha, et al., 2016. Modeling and forecasting energy consumption for residential buildings in Algeria using bottom-up approach. *Energy Build.* 121, 309–317.
- Ghofrani, Mahmoud, et al., 2011a. Smart meter based short-term load forecasting for residential customers. In: *North American Power Symposium (NAPS), 2011.* IEEE.
- Ghofrani, Mahmoud, et al., 2011b. Smart meter based short-term load forecasting for residential customers. In: *2011 North American Power Symposium.* IEEE.
- Habib, Salman, Kamran, Muhammad, Rashid, Umar, 2015. Impact analysis of vehicle-to-grid technology and charging strategies of electric vehicles on distribution networks—a review. *J. Power Sources* 277, 205–214.
- Hamzacebi, Coskun, Avni Es, Huseyin, 2014. Forecasting the annual electricity consumption of Turkey using an optimized grey model. *Energy* 70, 165–171.
- Hong, Tao, Fan, Shu, 2016. Probabilistic electric load forecasting: A tutorial review. *Int. J. Forecast.* 32 (3), 914–938.
- Hyndman, Rob J., Fan, Shu, 2010. Density forecasting for long-term peak electricity demand. *IEEE Trans. Power Syst.* 25 (2), 1142–1153.
- Jain, Rishu K., et al., 2014. Forecasting energy consumption of multi-family residential buildings using support vector regression: Investigating the impact of temporal and spatial monitoring granularity on performance accuracy. *Appl. Energy* 123, 168–178.
- Jovanović, Radiša Ž., Sretenović, Aleksandra A., Živković, Branislav D., 2015. Ensemble of various neural networks for prediction of heating energy consumption. *Energy Build.* 94, 189–199.
- Jung, Sang-Wook, Kim, Sahm, 2014. Electricity demand forecasting for daily peak load with seasonality and temperature effects. *Korean J. Appl. Statist.* 27 (5), 843–853.
- Kavousian, Amir, Rajagopal, Ram, Fischer, Martin, 2013. Determinants of residential electricity consumption: Using smart meter data to examine the effect of climate, building characteristics, appliance stock, and occupants' behavior. *Energy* 55, 184–194.
- Kaytez, Fazil, et al., 2015. Forecasting electricity consumption: A comparison of regression analysis, neural networks and least squares support vector machines. *Int. J. Electr. Power Energy Syst.* 67, 431–438.
- Lazos, Dimitris, Sproul, Alistair B., Kay, Merlinda, 2014. Optimisation of energy management in commercial buildings with weather forecasting inputs: A review. *Renew. Sustain. Energy Rev.* 39, 587–603.
- Li, Kangji, et al., 2019. A state of the art review on the prediction of building energy consumption using data-driven technique and evolutionary algorithms. *Build. Serv. Eng. Res. Technol.* 0143624419843647.
- Lindberg, K.B., Bakker, S.J., Sartori, I., 2019. Modelling electric and heat load profiles of non-residential buildings for use in long-term aggregate load forecasts. *Util. Policy* 58, 63–88.
- McCulloch, Warren S., Pitts, Walter, 1943. A logical calculus of the ideas immanent in nervous activity. *Bull. Math. Biophys.* 5 (4), 115–133.
- Ministry of Trade, Industry and Energy. 2017. The 8th basic plan for electric power supply and demand. Sejong: Korea.
- Pereira, Cesar Machado, de Almeida, Nival Nunes, Velloso, Maria L.F., 2015. Fuzzy modeling to forecast an electric load time series. *Procedia Comput. Sci.* 55, 395–404.
- Pielow, Amy, Sioshansi, Ramteen, Roberts, Matthew C., 2012. Modeling short-run electricity demand with long-term growth rates and consumer price elasticity in commercial and industrial sectors. *Energy* 46 (1), 533–540.
- Rahimi, Farrokh, Ipakchi, Ali, 2010. Demand response as a market resource under the smart grid paradigm. *IEEE Trans. Smart Grid* 1 (1), 82–88.
- Renn, Ortwin, Marshall, Jonathan Paul, 1950. Coal, nuclear and renewable energy policies in Germany: From the 1950s to the Energiewende. *Energy Policy* 99 (2016), 224–232.
- Reyna, Janet L., Chester, Mikhail V., 2017. Energy efficiency to reduce residential electricity and natural gas use under climate change. *Nature Commun.* 8, 14916.

- Ribeiro, Mauro, et al., 2018. Transfer learning with seasonal and trend adjustment for cross-building energy forecasting. *Energy Build.* 165, 352–363.
- Robert, Engle, 1982. Autoregressive conditional heteroscedasticity with estimates of the variance of United Kingdom inflation. *Econometrica*.
- Santamouris, M., et al., 2001. On the impact of urban climate on the energy consumption of buildings. *Sol. Energy* 70 (3), 201–216.
- Sigauke, C., Chikobvu, D., 2011. Prediction of daily peak electricity demand in South Africa using volatility forecasting models. *Energy Econ.* 33 (5), 882–888.
- Taskaya-Temizel, Tugba, Casey, Matthew C., 2005. A comparative study of autoregressive neural network hybrids. *Neural Netw.* 18 (5–6), 781–789.
- Taylor, James W., 2010. Triple seasonal methods for short-term electricity demand forecasting. *European J. Oper. Res.* 204 (1), 139–152.
- Taylor, James W., 2012. Short-term load forecasting with exponentially weighted methods. *IEEE Trans. Power Syst.* 27 (1), 458–464.
- Wang, Wei, et al., 2019. Forecasting district-scale energy dynamics through integrating building network and long short-term memory learning algorithm. *Appl. Energy* 248, 217–230.
- Winters, Peter R., 1960. Forecasting sales by exponentially weighted moving averages. *Manage. Sci.* 6 (3), 324–342.
- Xu, Ning, Dang, Yaoguo, Gong, Yande, 2017. Novel grey prediction model with nonlinear optimized time response method for forecasting of electricity consumption in China. *Energy* 118, 473–480.
- Yao, Albert W.L., Chi, S.C., Chen, J.H., 2003. An improved grey-based approach for electricity demand forecasting. *Electr. Power Syst. Res.* 67 (3), 217–224.
- Zhang, Fan, et al., 2016. Time series forecasting for building energy consumption using weighted Support Vector Regression with differential evolution optimization technique. *Energy Build.* 126, 94–103.